Available online at www.sciencedirect.com
ScienceDirect
Trans. Nonferrous Met. Soc. China 20(2010) 2192−2197
Transactions of Nonferrous Metals Society of China
www.tnmsc.cn

Surface modification of TC4 Ti alloy by laser cladding with TiC+Ti powders

ZHANG Ke-min(张可敏)[1], ZOU Jian-xin(邹建新)[2], LI Jun(李 军)[1],
YU Zhi-shui(于治水)[1], WANG Hui-ping(王慧萍)[1]

1. School of Materials Engineering, Shanghai University of Engineering Science, Shanghai 201620, China;
2. National Engineering Research Center of Light Alloy Net Forming,
School of Materials Science and Engineering, Shanghai Jiao Tong University, Shanghai 200240, China

Received 23 October 2009; accepted 15 August 2010

Abstract: Laser surface cladding was applied on a TC4 Ti alloy to improve its surface properties. Mixed TiC and Ti powders with a TiC-to-Ti mass ratio of 1:3 were put onto the TC4 Ti alloy and subsequently treated by laser beam. The microstructure and composition modifications in the surface layer were carefully investigated by using SEM, EDX and XRD. Due to melting, liquid state mixing followed by rapid solidification and cooling, a layer with graded microstructures and compositions formed. The TiC powders were completely dissolved into the melted layer during melting and segregated as fine dendrites when solidified. The inter-dendritic areas were filled with fine α' phase lamellae enrich in Al. Mainly due to the reduced TiC volume fraction with increasing depth, the hardness decreases with increasing depth in the laser clad layer with a maximum value of HV1400, about 4.5 times of the initial one.

Key words: TC4 Ti alloy; TiC; laser cladding; segregation; hardness

1 Introduction

Ti alloys are widely used in industries due to a good combination of their mechanical and chemical properties, such as high stiffness, low density and good corrosion resistance. However, Ti alloys often suffer from poor wear resistance owing to their relatively low hardness which hinders its further application[1−3]. In many cases, the failure of a material starts from its surface, especially under wear and corrosion environment. Therefore, it is essential to improve the wear resistance of Ti alloys using surface modification with the aim of improving their global performance. Different surface treatment techniques, for instances, physical vapor deposition, chemical vapor deposition, sol-gel methods, anodic oxidation and so on, have been applied on Ti alloys in order to improve their wear or corrosion resistances[2, 4−5]. Nevertheless, these methods have their own limitations. For example, the films deposited onto Ti alloys are often very thin and suffer from poor adhesion with the substrate.

Among all kinds of surface treatment techniques, laser cladding offers an optimum approach to obtain a thick layer onto a material with superior properties. By laser cladding, different alloys or metal matrix composites can be easily produced onto treated material surfaces with strong metallurgical bonding between the clad layer and the substrate[3, 6−7]. Considering the advantages mentioned above, laser cladding is used in the present work to fabricate an in-situ metal matrix composite onto a TC4 Ti alloy to harden the surface layer. The microstructure and composition modifications in the laser clad layer are investigated in detail.

2 Experimental

2.1 Sample preparation and laser treatment

The titanium alloy investigated here is commercially available TC4 alloy which was solution

Foundation item: Project(J51402) supported by the Leading Academic Discipline Project of Shanghai Education Commission, China; Project(gjd08004) supported by the Foundation for Excellent Youth Scholar of China; Project(08QA14035) supported by the Shanghai Science and Technology Development Foundation, China; Project(0852nm01400) supported by the Special Foundation of Shanghai Education Commission for Nano-Materials Research, China; Project(08520513400) supported by Crucial Project of the Shanghai Science and Technology Commission, China

Corresponding author: LI Jun; Tel: +86-21-67791203; E-mail: Jacob_lijun@sina.com

DOI: 10.1016/S1003-6326(09)60441-6

treated at 1 100 °C and subsequently quenched in water. Its nominal chemical composition is as follows: 6.5% Al, 4.26% V and balance Ti (mass fraction). Samples for laser treatment were cut into small coupons (15 mm×15 mm×10 mm) from a 10 mm-thick sheet. All the samples were ground with sand papers, polished down to diamond paste of 1.5 μm and ultrasonically cleaned in acetone prior to the laser treatments. Fig.1 shows a typical SEM image taken on the untreated sample under backscattered electron condition. The initial material contains a fine lamellar α' grain structure (the width is about 3 μm) in very large areas. These domains are actually β phase grains present at high temperature and transferred into α'-Ti during cooling.

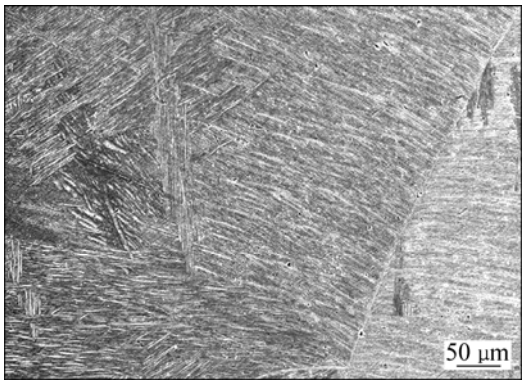

Fig.1 SEM image of untreated TC4 sample

Prior to the laser treatment, mixed TiC and Ti powders with a TiC-to-Ti mass ratio of 1:3 were put onto the TC4 sample. The powder layer was then pressed in order to remove the gas between powder particles. The total depth of the powder layer is around 500 μm. The laser cladding treatment was carried out using a HL-2000 type CO_2 laser source. The beam cross section (shape and area), beam power and scanning speed are the main parameters to be adjusted. For the present study, these parameters were set as 5 mm, 3 500 W and 2 mm/s, respectively.

2.2 Characterizations of laser clad layer

The phases present on the surface of the treated sample were analyzed by X-ray diffraction (XRD) using a Shimadzu D−6000 goniometer operating with Cu K_α radiation. The microstructure of the treated samples was observed from cross section by using optical microscopy (OM) and a Hitachi 3000 scanning electron microscopy (SEM) equipped with an electron dispersion X-ray spectroscopy (EDX).

Modifications of the composition within the laser clad layers were investigated by EDX analysis at different depth. Vicker's hardness of the cross section was measured under load of 3 N.

3 Results

3.1 Cross sectional microstructure and phase identification

Fig.2 shows OM and SEM images illustrating the aspects of the laser clad layer in a cross sectional view. Fig.2(a) shows the overall morphology of the melted layer, which has a curved shape depressing toward the substrate. It has been established that the shape of the laser clad layer mainly depends on its wettability with regard to the substrate[8−9]. In the present study, it is obvious that the laser clad layer has good wettability with the substrate as they both contain Ti phase. The depth of the laser clad layer is around 1.5 mm. Within this laser clad layer, very fine dendritic structure can be seen clearly, which corresponds to the TiC phase[10]. Fig.2(b) gives more details of the microstructure present in the melted layer. It can be seen that beside the TiC dendrites, there are also fine needle structures distributing among those TiC dendrites.

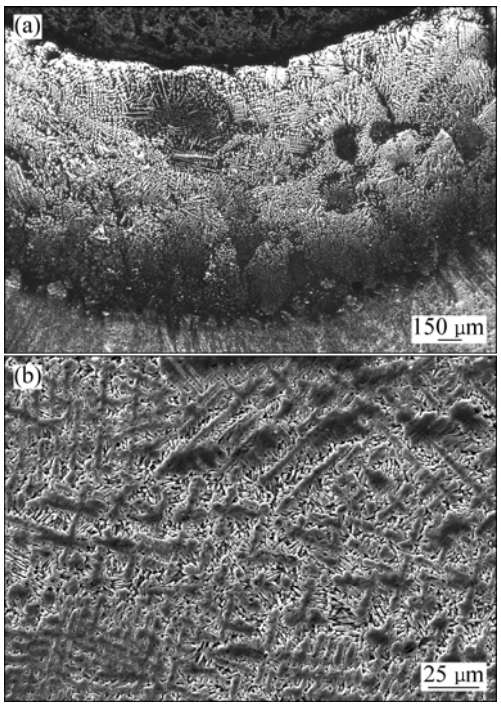

Fig.2 OM (a) and SEM (b) images of laser clad TC4 sample

Fig.3 shows XRD patterns recorded from the untreated and treated samples at different depths. The XRD pattern of the initial sample shows peaks only corresponding to the α-Ti phase, the peaks coming from TiC phase appears after the laser treatments. The peaks belonging to α phase broadens significantly after the laser cladding treatment. Such a peak broadening together with the existence of fine needles in the inter-dendritic areas as shown in Fig.2(b), indicates the formation of α' martensite in the laser clad layer. It can

be also concluded by comparing the XRD patterns measured on the sample surface (Fig.3(b)) and subsurface (Fig.3(c)), the relative diffraction intensity between TiC and α'-Ti decreases when approaching the substrate, which means that the fraction of TiC phase decreases when the depth increases.

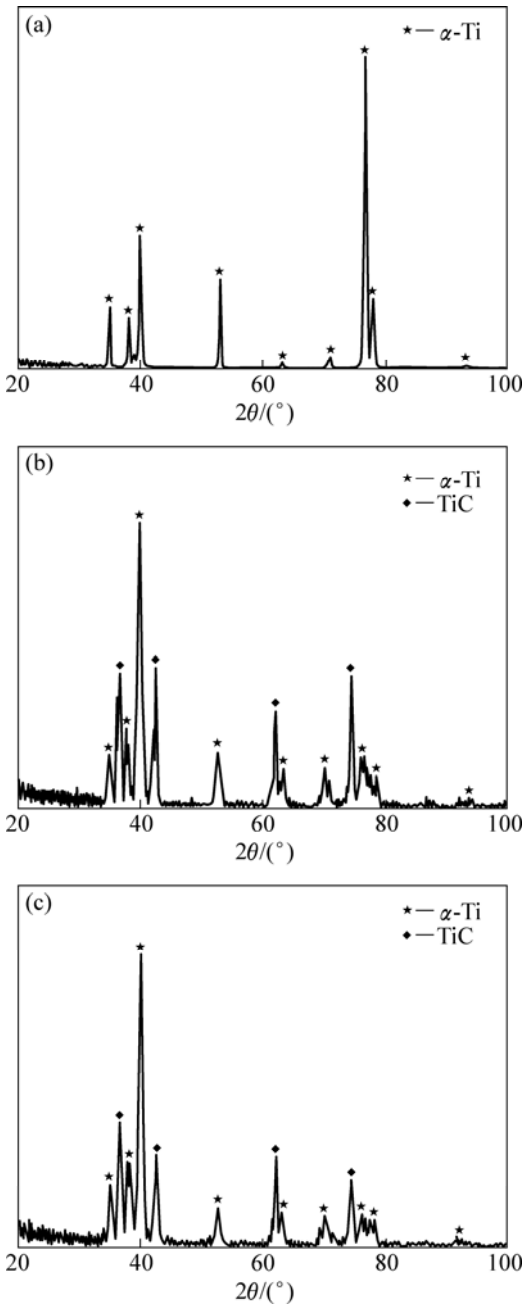

Fig.3 XRD patterns of untreated sample (a), top surface layer (b) and subsurface of laser clad sample (c)

3.2 Through-depth characterization of laser clad layer

Fig.4 shows the cross-section morphology of the top surface layer and the corresponding element distribution map of Al. It is worth noting that the distribution maps of other elements (Ti, V and C) look quite "homogeneous" as the signals recorded, for these elements are either too strong (Ti) or too weak (V and C). Therefore, only Al distribution is shown here. From Figs.4(a) and (b), the mass fraction of Al is quite heterogeneous and seems to distribute only between the TiC dendrites. In other words, Al stays mainly in the α-Ti. By the comparison of all the figures, three distinct features can be observed: 1) the TiC dendrites become finer when the depth increases; 2) the volume fraction of TiC dendrites decreases with increasing depth; 3) the distribution of Al becomes more homogeneous when approaching the substrate.

The composition analysis along depth is carried out by using EDX and the results are summarized in Fig.5. The mass fractions of Al, V and C are plotted as a function of the depth. It should be noted that EDX is not an accurate method to obtain precise element concentrations. Therefore, the profiles only reflect the trend of element distribution along depth. It is seen in Fig.5 that the C mass fraction decreases gradually with increasing depth within the laser clad layer and drops down very quickly at the melt/substrate interface. The Al and V mass fraction show very similar trend, which indicates that they keep nearly constant in the middle laser clad layer, drop down on the top surface layer and increase at the interface layer.

3.3 Cross section microhardness of laser clad layer

Fig.6 shows the evolution of the microhardness with depth for the laser treated sample. The initial microhardness of the TC4 alloy, about HV 300, is considered as the microhardness of substrate side when the depth is higher than 1 500 μm. It is clear from the hardness profile that a significant hardening is induced by the laser cladding in the surface layer. The hardness increases to about HV 1 400 on the top surface, which is about 4.5 times of the initial hardness. It then decreases gradually when approaching the substrate.

4 Discussion

When a laser beam is applied on the surface of a material, it always induces many phenomena, such as fast heating, melting, liquid mixing, convection and resolidification[8, 11]. These phenomena determine the final microstructure and properties of the laser clad layer. However, the thermal history at different depths is very different, leading to the formation of a microstructure and composition graded layer after laser treatment. In this case, the complex cladding process can be described as shown in Fig.7.

First, a thick Ti+TiC powder layer is pre-coated onto the TC4 alloy substrate, as shown in Fig.7(a). At the early stage of the laser treatment, Ti particles at the top surface layer are melted prior to the TiC particle, hence,

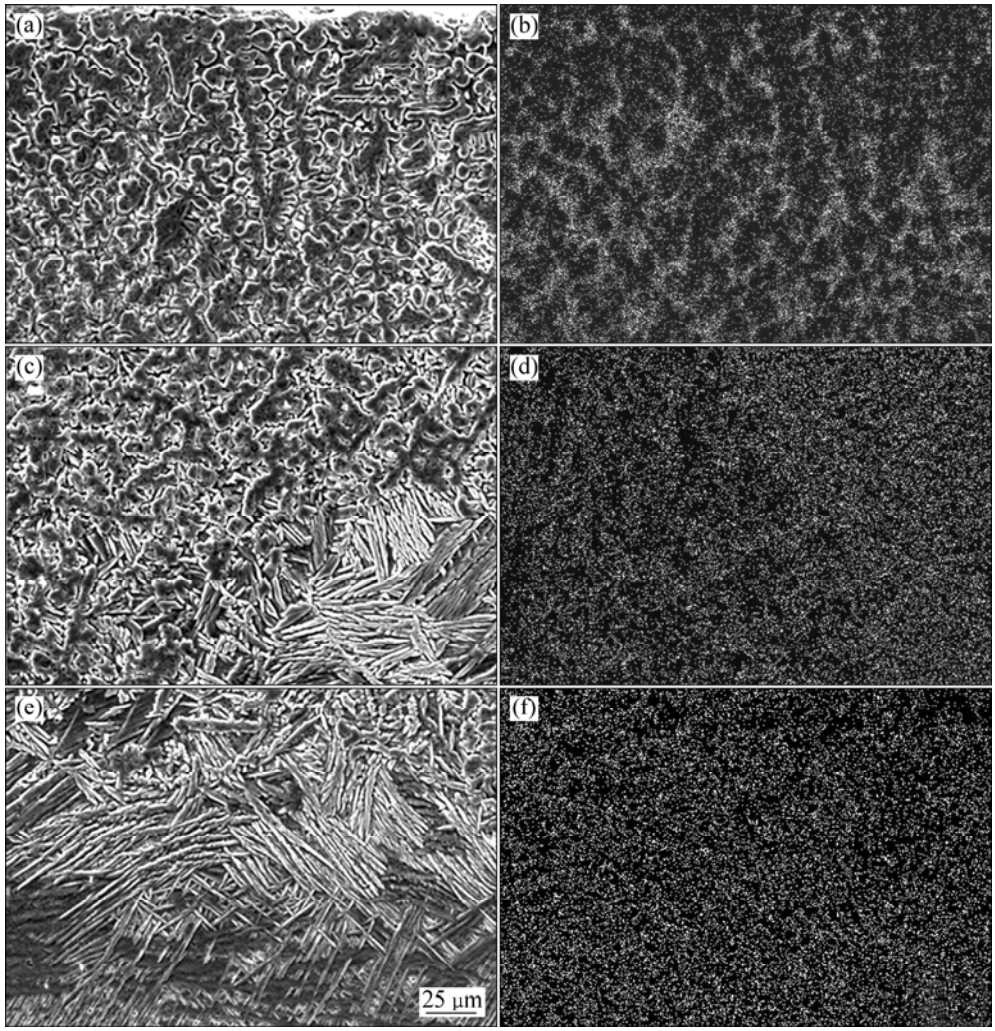

Fig.4 SEM images of laser clad layer at different depths (a, c, e) and corresponding Al distribution map (b, d, f): (a, b) Top surface; (c, d) Subsurface at about 750 μm; (e, f) Subsurface at melt/substrate interface

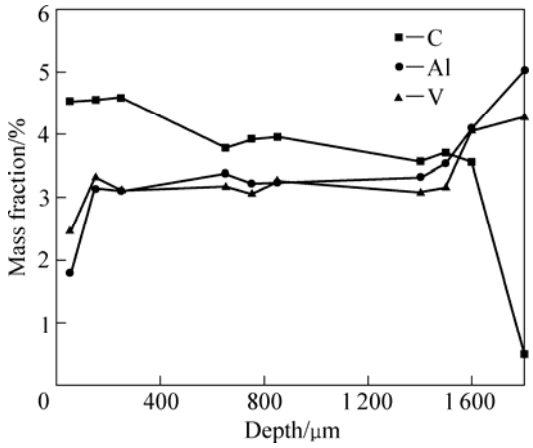

Fig.5 Composition distribution profiles of C, Al and V as function of depth measured by EDX

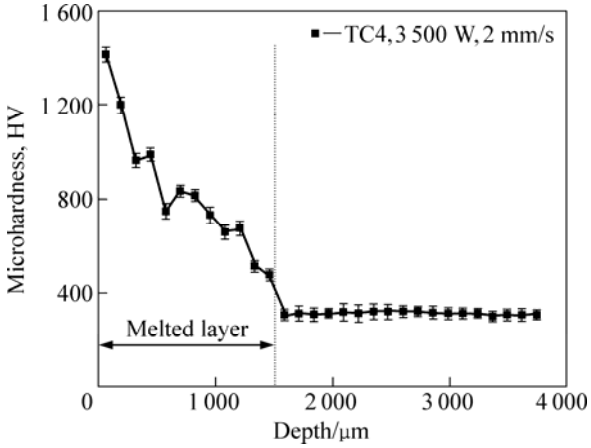

Fig.6 Microhardness profile along depth of laser clad sample

Ti has a lower melting point than that of TiC[12]. When this process continues, TiC particles start to be dissolved into Ti melt[13]. After the whole powder layer is melted, a part of the matrix will also be included into the laser clad layer due to the continuous laser power input [14]. A composition gradient is established at this stage, especially at the bottom of the melt close to the matrix,

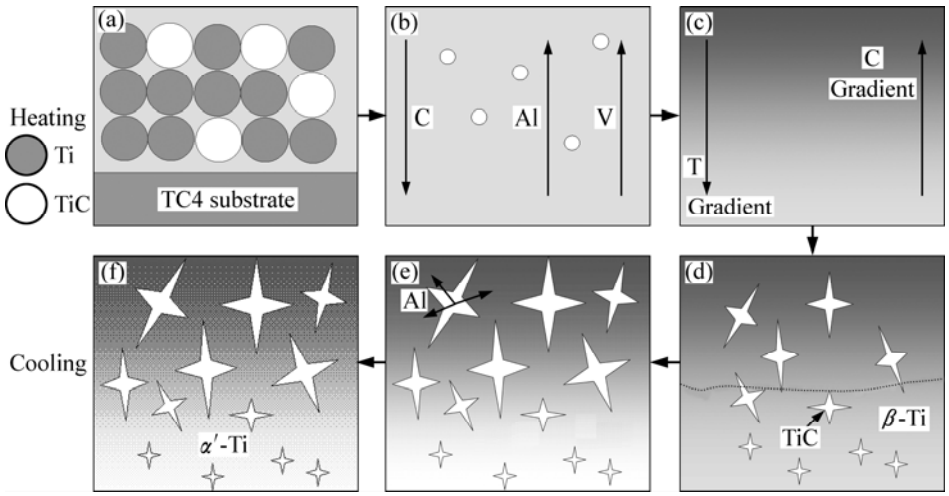

Fig.7 Schematic illustrations showing microstructure evolution in surface layers during laser cladding

as shown in Fig.7(b). The C atoms diffuse toward the bottom while Al and V atoms move from the melted matrix to the top surface layer due to the laser induced convection in the melt. However, the melt dwell time is not long enough so that the composition gradient still exists before solidification starts, which is illustrated in Fig.7(c). During the cooling stage, the solidification initiates from the melt/substrate interface due to the heat conduction toward matrix[12]. At the early stage of the solidification process, TiC nuclei form prior to the Ti nuclei[14]. They grow larger and larger until the local temperature decreases to a certain value at which the β-Ti phase nucleation occurs[15], as shown in Fig.7(d). The melt undergoes such a process until all the liquid is consumed. As the cooling rate at the solidification front decreases when it moves toward the surface [12], the melt duration increases from the bottom to the top. Consequently, TiC dendrites have more time to grow on the top surface layer than those in the bottom of the melt. On the other hand, since the solubility of Al in TiC is very limited, the Al atoms are pushed out from TiC dendrites and remain in the rest of liquid, as shown in Fig.7(e). Therefore, α'-Ti formed between Ti dendrites are rich in Al. Such segregation behaviour of Al depends on the local cooling rate. When the cooling rate increases, the segregation is suppressed due to a "solute trapping effect"[16]. Consequently, Al concentration becomes more homogeneous with increasing depth owning to the increasing cooling rate. Considering the factors above, a laser clad layer with graded microstructure and composition forms in the end, as illustrated in Fig.7(d).

The hardness of the laser clad layer is determined both by the volume fraction and the size of TiC dendrites as TiC is very hard and plays the major role for the increased hardness[10, 13]. The higher the TiC volume fraction is, the higher the hardness is. In contrast, the finer the TiC dendrites is, the higher the hardness is. However, the volume fraction decreases with depth while the size of the dendrites decreases with depth, too. In this case, the decreased hardness with depth indicates that the volume fraction of the TiC accounts for the major local hardness value in the laser clad layer.

5 Conclusions

1) Mixed TiC and Ti powders with a TiC-to-Ti mass ratio of 1:3 were put onto the TC4 samples and subsequently treated by laser beam. It was observed that a layer with graded microstructures and compositions formed on the matrix due to the melting, liquid state convection followed by rapid solidification and cooling.

2) TiC powders were completely dissolved into the melted layer during melting and segregated as fine dendrites when solidified. The inter-dendritic areas were filled with fine α'-Ti lamellae.

3) Both the size and volume fraction of TiC dendrites decrease with increasing depth, while the distribution of Al becomes more homogeneous.

4) As a consequence of the reduced TiC volume fraction with increasing depth, the hardness decreases with depth in the laser clad layer with a maximum value of HV 1 400 on the top surface, which is about 4.5 times of the initial one.

References

[1] LIU Dao-xin, TANG Bin, ZHU Xiao-dong, CHEN Hua, HE Jia-wen, CELIS J P. Improvement of the fretting fatigue and fretting wear of Ti6Al4V by duplex surface modification [J]. Surface and Coatings Technology, 1999, 116/119(9): 234−238.

[2] HAGER C H J, SANDERS J H, SHARMA S. Unlubricated gross slip fretting wear of metallic plasma-sprayed coatings for Ti6Al4V surfaces [J]. Wear, 2008, 265(3/4): 439−451.

[3] PANG W, MAN H C, YUE T M. Laser surface coating of Mo–WC metal matrix composite on Ti6Al4V alloy [J]. Materials Science and

Engineering A, 2005, 390(1/2): 144−153.

[4] VARIOLA F, YI J H, RICHERT L, JWUEST J D, ROSEI F, NANCI A. Tailoring the surface properties of Ti6Al4V by controlled chemical oxidation [J]. Biomaterials, 2008, 29(10): 1285−1298.

[5] SILVA M M, UEDA M, PICHON L, REUTHER H, LEPIENSKI C M. Surface modification of Ti6Al4V alloy by PIII at high temperatures: Effects of plasma potential [J]. Nuclear Instruments and Methods in Physics Research B, 2007, 257(1/2): 722−726.

[6] ALEMOHAMMAD H, ESMAEILI S, TOYSERKANI E. Deposition of Co-Ti alloy on mild steel substrate using laser cladding [J]. Materials Science and Engineering A, 2007, 456(1/2): 156−161.

[7] KHOSROSHAHI M E, MAHMOODI M, TAVAKOLI J. Characterization of Ti6Al4V implant surface treated by Nd:YAG laser and emery paper for orthopaedic applications [J]. Applied Surface Science, 2007, 253(21): 8772−8781.

[8] CAI Li-fang, ZHANG Yong-zhong, SHI Li-kai. Microstructure and formation mechanism of titanium matrix composites coating on Ti-6Al-4V by laser cladding [J]. Rare Metals, 2007, 26(4): 342-346.

[9] MAJUMDAR J D, MANNA I, KUMAR A. Direct laser cladding of Co on Ti-6Al-4V with a compositionally graded interface [J]. Journal of Materials Processing Technology, 2009, 209(5): 2237−2243.

[10] PU Yu-ping, GUO Bao-gang, ZHOU Jian-song. Microstructure and tribological properties of in situ synthesized TiC, TiN, and SiC reinforced Ti3Al intermetallic matrix composite coatings on pure Ti by laser cladding [J]. Applied Surface Science, 2008, 255(5): 2697−2703.

[11] LI Li-qun, LIU De-jian, CHEN Yan-bin, WANG Chun-ming, LI Fu-quan. Electron microscopy study of reaction layers between single-crystal WC particle and Ti-6Al-4V after laser melt injection [J]. Acta Materialia, 2009, 57(12): 3606−3614.

[12] YANG Yu-ling, ZHANG Duo, LIU Chang-sheng, YANG Yi-ran. Laser cladding of TiCN/Ti coatings on Ti6-Al4-V and the calculation of the temperature field [J]. Optical Engineering, 2008, 47(8): 084301−5.

[13] YANG Yu-ling, ZHANG Duo, YAN Wei, ZHENG Yi-ran. Microstructure and wear properties of TiCN/Ti coatings on titanium alloy by laser cladding [J]. Optics and Lasers in Engineering, 2010, 48(1): 119−124.

[14] BRIAN C L, SHAHRZAD E. In-situ laser-fabrication and characterization of TiC-containing Ti-Co composite on pure Ti substrate [J]. Journal of Alloys and Compounds, 2009, 482(1/2): 246−252.

[15] SUN R L, LEI Y W, NIU W. Laser clad TiC reinforced NiCrBSi composite coatings on Ti–6Al–4V alloy using a CW CO_2 laser [J]. Surface and Coatings Technology, 2009, 203(10/11): 1395−1399.

[16] BOETTINGER W J, CORIELL S R, GREER A L, KARMA A, KURZ W, RAPPAZ M, TRIVEDI R. Solidification microstructures: recent developments, future directions [J]. Acta Materialia, 2000, 48(1): 43−70.

(Edited by FANG Jing-hua)